Available online at www.sciencedirect.com
SCIENCE DIRECT®
Tectonophysics 364 (2003) 1–8
TECTONOPHYSICS
www.elsevier.com/locate/tecto

Progress in microboudin method for palaeo-stress analysis of metamorphic tectonites: application of mathematically refined expression

Toshiaki Masuda*, Nozomi Kimura, Yuko Hara

Institute of Geosciences, Shizuoka University, 836 Oya, Shizuoka 422-8529, Japan

Received 9 July 2002; accepted 31 January 2003

Abstract

The microboudin method for palaeo-stress analysis is mathematically refined by incorporating the recently proposed shear-lag model, which describes the relationship between stress distribution along a fibre embedded within an elastic matrix and the far-field differential stress applied to the matrix. The refined probability density function of fractured fibres (G) with respect to the aspect ratio of the fibre (r) and the stress parameter (λ) is given by

$$G(r,\lambda) = 1 - \exp\left[-\frac{m-1}{m} r\lambda^m \left(\frac{E_f}{E_q}\right)^m \left\{1 - \left(1 - \frac{E_q}{E_f}\right)\frac{1}{\cosh(Ar)}\right\}^m\right]$$

where E_q and E_f are the elastic constants of the matrix and fibre, m is the Weibull modulus of the fibre material, and A is a constant. The stress parameter λ is defined as $\lambda = \sigma_0/S^*$, where σ_0 is the far-field differential stress applied to the matrix and S^* is the modal fracture strength of the fibre material at $r = 1$. This method is applied to tourmaline and piemontite boudins in quartzose rocks from six areas, and it is revealed that the probability density function adequately models the proportion of boudinaged tourmaline and piemontite grains. The value of λ is determined for each sample, allowing σ_0 to be determined by this method when S^* is known.

Keywords: Microboudin structure; Tourmaline; Piemontite; Quartz; Palaeo-stress; Metamorphic tectonites

1. Introduction

Determination of the magnitude of stress during orogenesis is an important aspect of structural geology (e.g., Hobbs et al., 1976). In the early 1980s, several authors (e.g., Weathers et al., 1979; Etheridge and Wilkie, 1981; Ord and Christie, 1984) attempted to estimate the magnitude of differential stress acting on plastically deformed rocks based on the grain size and dislocation density palaeopiezometers proposed by Mercier et al. (1977) and Twiss (1986), respectively. These methods, originally derived for metallurgical purposes (e.g., Sellars, 1978), assume steady state deformation. However, steady state deformation is not likely to occur in nature. The process that most degrades the performance of these palaeopiezometers is post-deformation annealing, during which grain size

* Corresponding author. Fax: +81-54-237-9895.
E-mail address: setmasu@ipc.shizuoks.ac.jp (T. Masuda).

0040-1951/03/$ - see front matter © 2003 Elsevier Science B.V. All rights reserved.
doi:10.1016/S0040-1951(03)00045-3

and dislocation density will be altered significantly. Thus, these methods seem unsuitable for natural deformation (e.g., White et al.,1980).

Two other methods have been proposed from a geological viewpoint (e.g., Passchier and Trouw, 1996): the calcite-twin method (e.g., Jamison and Spang, 1976; Rowe and Rutter, 1990; Lacombe, 2001), and the microboudin method (Masuda et al., 1989, 1990). The calcite-twin method is applicable to weakly metamorphosed marbles and gives the absolute magnitude of differential stress, whereas the microboudin method is applicable to schists and gneisses with mineral boudins and gives the relative magnitude of differential stress during retrograde metamorphism. The present paper refines the microboudin method by incorporating a recently proposed shear-lag model (e.g., Taya and Arsenault, 1989; Zhao and Ji, 1997) for the stress distribution along the fibre. The potential of the microboudin method for estimation of the absolute magnitude of differential stress is also discussed.

2. Outline of existing microboudin method

The microboudin method consists of two independent parts: measurement of the proportion of boudinaged grains embedded in a matrix, and theoretical prediction of the proportion as a function of differential stress (Masuda et al., 1989, 1990). Piemontite boudins were selectively analysed in Masuda et al. (1989, 1990), but other columnar minerals such as tourmaline, alkali-amphiboles, rutile and apatite also form good microboudin structures in many schists and are potentially analysable. The most common matrix for microboudins is quartz, but calcite also encapsulates microboudins. The relative magnitude of differential stress is determined by comparing the theoretical and measured proportions of boudinaged grains (Masuda et al., 1989). As the measurement of boudinaged grains does not require improvement, we concentrate here on the refinement of theoretical prediction.

Masuda et al. (1989) proposed the expression

$$G(r,B) = 1 - \exp\left[-\frac{m-1}{m} rB^m \left\{1 - \frac{1}{\cosh(\alpha r)}\right\}^m\right] \quad (1)$$

for the proportion of boudinaged fibrous grains (G) as a function of the aspect ratio of the fibre (r) and a dimensionless parameter (B). B is defined as

$$B = \frac{E_f}{E_q}\frac{\sigma_0}{S^*} \quad (2)$$

where E_q and E_f are the elastic moduli of the matrix mineral and fibre mineral, S^* is the average fracture strength of the fibre mineral at $r=1$, and σ_0 is the far-field differential stress. Thus, B is proportional to σ_0. The parameters m and α in Eq. (1) are the Weibull modulus of the fibre and a constant that will be shown later.

Eq. (1) is derived from two mechanical considerations. One is the stress-transfer model (e.g., Lloyd et al., 1982; Kelly, 1973), which gives the relationship between the far-field strain (ε) and the tensile stress (σ)

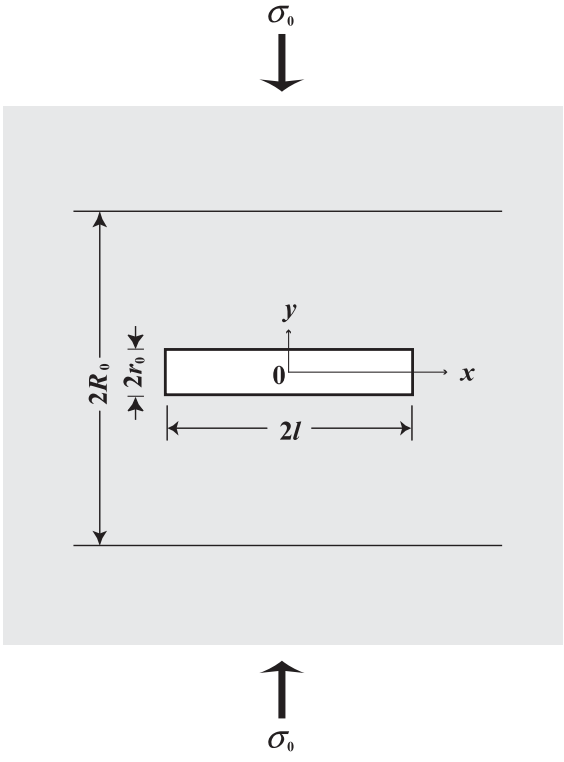

Fig. 1. Setting of fibre deformation surrounded by a homogeneous elastic matrix after Zhao and Ji (1997). σ_0 = far-field differential stress; $2l$ = length of fibre; $2r_0$ = diameter of fibre; and $2R_0$ = length of unit cell. Coordinate axes x and y are indicated.

transferred to the fibre material at position x (Fig. 1) as follows.

$$\sigma = E_f \varepsilon \left[1 - \frac{\cosh(\delta x)}{\cosh(\delta l)}\right] \quad (3)$$

where l is the half-length of the fibre, and δ is given by

$$\delta = \frac{1}{w}\left[\frac{2\pi G_m}{E_f \ln(R/r_0)}\right]^{1/2} \quad (4)$$

where w is the width of the fibre, G_m is the shear modulus of the matrix, and R and r_0 are the mean distances between adjacent fibres and the fibre radius. Masuda et al. (1989, 1990) assumed that fracturing occurs at the centre of the fibre ($x=0$), and substituted the stress–strain relationship of the elastic matrix ($\varepsilon=\sigma_0/E_q$). They obtained the relationship between the far-field differential stress (σ_0) and transferred differential stress (σ) at the centre of the fibre as follows.

$$\sigma = \frac{E_f}{E_q}\sigma_0\left[1 - \frac{1}{\cosh(\alpha r)}\right] \quad (5)$$

where $\alpha r = \delta l$.

The other mechanical consideration is associated with the fracture strength of the fibre material. The fracture strength is a statistical parameter that is usually well represented by the Weibull distribution (e.g., Lawn, 1993). S^* represents the average of the distribution, whereas m (the Weibull modulus) is related to the standard deviation (e.g., Fig. 13 of Masuda et al., 1989). Masuda et al. (1989) applied the weakest-link theory (Weibull, 1939; Epstein, 1948) for the fracturing of fibre minerals, and derived the probability density function of fracture strength $g(r,\sigma)$ as a function of aspect ratio (r) and applied stress (σ) to give

$$g(r,\sigma) = \frac{(m-1)}{(S^*)^m} r\sigma^{m-1}\exp\left[-\frac{m-1}{m} r\left(\frac{\sigma}{S^*}\right)^m\right] \quad (6)$$

They also derived the cumulative distribution function $G(r,\sigma)$ as follows.

$$G(r,\sigma) = \int_0^\sigma g(r,\sigma)\mathrm{d}\sigma = 1 - \exp\left[-\frac{m-1}{m} r\left(\frac{\sigma}{S^*}\right)^m\right] \quad (7)$$

Eq. (1) is derived by substituting Eq. (5) into Eq. (7).

3. Refined expression for proportion of boudinaged grains

The stress-transfer model depicted by Eq. (5) appears inappropriate when we consider the stress for the special case $E_q = E_f$. A homogeneous stress distribution along the fibre ($\sigma = \sigma_0$) is expected in this case, but such a stress distribution cannot be represented by Eq. (5). Recently, Zhao and Ji (1997) presented a new model (shear-lag model) for stress distribution along a fibre (Fig. 1) following a review

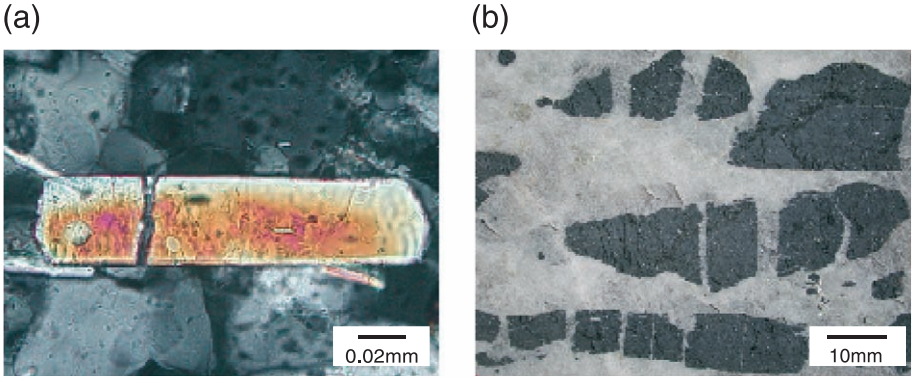

Fig. 2. Micrographs of analysed samples. (a) Wadi Tayin. A boudinaged tourmaline grain in a quartz matrix (crossed-polarized light). (b) Greenbushes. Tourmaline grains scattered in a quartzose matrix.

of the literature on materials science (e.g., Taya and Arsenault, 1989). They referred to the equation:

$$\sigma = E_f \varepsilon \left[1 - \left(1 - \frac{E_q}{E_f}\right) \frac{\cosh(\beta x)}{\cosh(\beta l)}\right] \quad (8)$$

where

$$\beta = \frac{r}{l}\left[\frac{E_q}{E_f(1+\nu_m)\ln(R_0/r_0)}\right]^{1/2} \quad (9)$$

and ν_m is the Poisson's ratio of the matrix, and R_0 and r_0 are the radii of the unit cell and fibre. Eq. (8) satisfies $\sigma = \sigma_0$ at any x when $E_q = E_f$. As the stress in the fibre is well represented by that at the centre (Zhao and Ji, 1997), by substituting $x = 0$, we obtain

$$\sigma = \frac{E_f}{E_q}\sigma_0 \left[1 - \left(1 - \frac{E_q}{E_f}\right) \frac{1}{\cosh(Ar)}\right] \quad (10)$$

where

$$A = \frac{\beta l}{r} = \left[\frac{E_q}{E_f(1+\nu_m)\ln(R_0/r_0)}\right]^{1/2} \quad (11)$$

In this derivation, we use the relationship between stress and strain of the elastic matrix, $\varepsilon = \sigma_0/E_q$.

Eq. (10) appears more comprehensive than Eq. (5). By substituting Eq. (10) into Eq. (7), we obtain the following new expression for the probability density of fractured fibres.

$$G(r,\lambda) = 1 - \exp\left[-\frac{m-1}{m} r \lambda^m \left(\frac{E_f}{E_q}\right)^m \times \left\{1 - \left(1 - \frac{E_q}{E_f}\right)\frac{1}{\cosh(Ar)}\right\}^m\right] \quad (12)$$

where λ is a new parameter defined as

$$\lambda = \frac{\sigma_0}{S^*} \quad (13)$$

The parameter λ is a stress parameter, proportional to σ_0.

4. Analysed samples and proportion of boudinaged grains

We reanalysed piemontite microboudins of four samples previously analysed in Masuda et al. (1989) and two additional samples from Greenbushes and Wadi Tayin using the refined Eq. (12). The Greenbushes sample (Fig. 2b) is a pegmatite of the Yilgarn craton, Western Australia (Partington, 1990), in which columnar, centimeter-scale tourmaline grains are boudinaged within a quartzose matrix. The age of pegmatite deformation is inferred to be the latest Archaean (Partington, 1990). The Wadi Tayin sample (Fig. 2a) was collected from the metamorphic sole beneath the Samail ophiolite in the Sultanate of Oman (Boudier and Coleman, 1981; Hacker and Mosenfelder, 1996), and contains tourmaline grains of 10–100 μm in size. Deformation/metamorphism is inferred to have been caused by emplacement of hot mantle peridotites during the initial stage of closure of Tethys during the late Cretaceous intraoceanic thrusting event (e.g., Boudier and Coleman, 1981; Hacker et al., 1996).

In the same procedure as shown in Masuda et al. (1989, 1990), we measured the length of each microboudins and interboudin gaps if the tourmaline grains were pulled apart (Fig. 3). Width was also measured for such grains. The aspect ratio of the tourmaline grains at the time of fracturing was calculated using the strain-reversal method proposed by Ferguson (1981). For intact tourmaline grains, we simply measured the

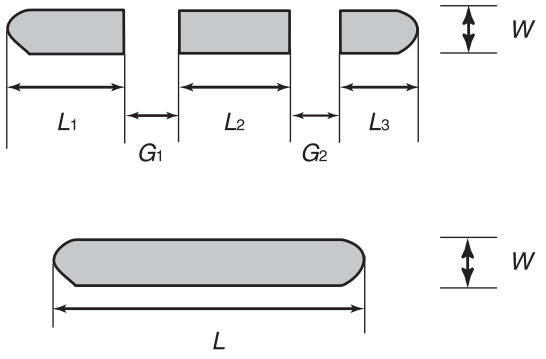

Fig. 3. Measurement of microboudinaged grains (top) and intact grains (bottom). L = length; W = width. The aspect ratio r is calculated by $r = L/W$. L in the top grain is calculated by $L = \Sigma L_i$. L_i and G_i are used to restore the history of microbuodinage by the strain reversal method (Ferguson, 1981).

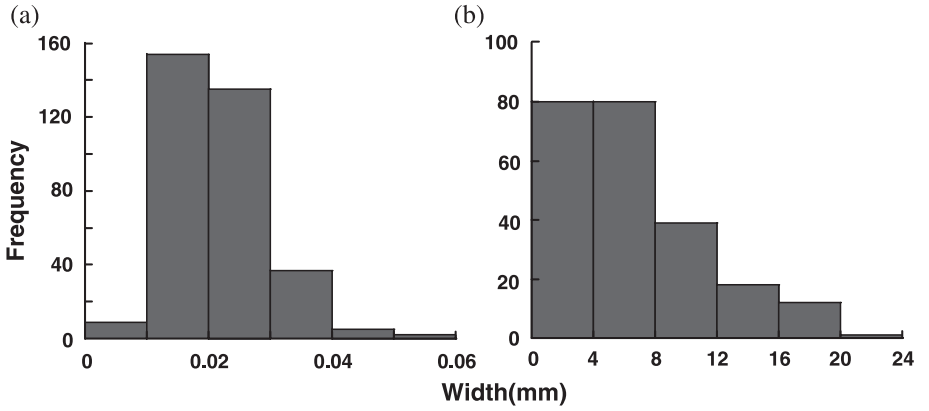

Fig. 4. Frequency distribution of width of tourmaline grains in Wadi Tayin (a) and Greenbushes (b) samples. Note that the widths of tourmaline in the two samples significantly differ.

length and width. Fig. 4 shows the grain size distribution of tourmaline grains. The numbers of boudinaged and intact grains with respect to the aspect ratio are shown in Fig. 5, and the proportions of boudinaged grains are plotted in Fig. 6 for further analysis.

5. Fitting theoretical curves to the measured data

We assume that fracturing of mineral fibres (tourmaline and piemontite) occurs when the transferred stress in the fibre (σ) becomes equal to the fracture strength of the fibre. We also assume no size effects on the fracture strength of tourmaline and piemontite. $G(r, \lambda)$ in Eq. (12), the theoretical probability density function of fracture strength, is then compared with $M(r)$, the measured proportion of boudinaged grains at r (see Masuda et al., 1989). The parameter λ can be determined by a least-squares fit so as to minimise $T(\lambda)$ as follows.

$$T(\lambda) = \sum_{r} \left[G(r, \lambda) - M(r)\right]^2 \tag{14}$$

However, our situation is not so simple.

$G(r, \lambda)$ is influenced by four constants: E_q, E_f, m and A. We can obtain appropriate values for E_q, E_f and A as follows. We consulted Simmons and Wang (1971) for E_q and E_f at room temperature and pressure (not high temperature and pressure). However, as the influence of temperature and pressure on the ratio of E_q to E_f appears negligible (see Masuda et al., 1995), we use the values measured under room conditions. The constant A is given as 0.5 and 0.4 for piemontite and tourmaline, respectively. These values are derived

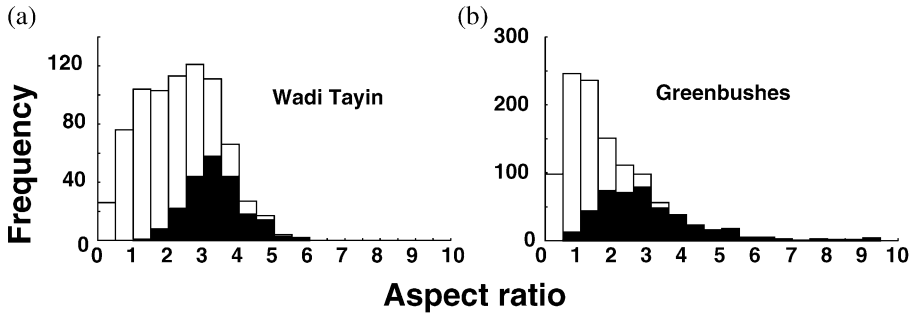

Fig. 5. Frequency distribution of aspect ratio of boudinaged and intact grains in Wadi Tayin (a) and Greenbushes (b) samples. Boudinaged grains are indicated in black.

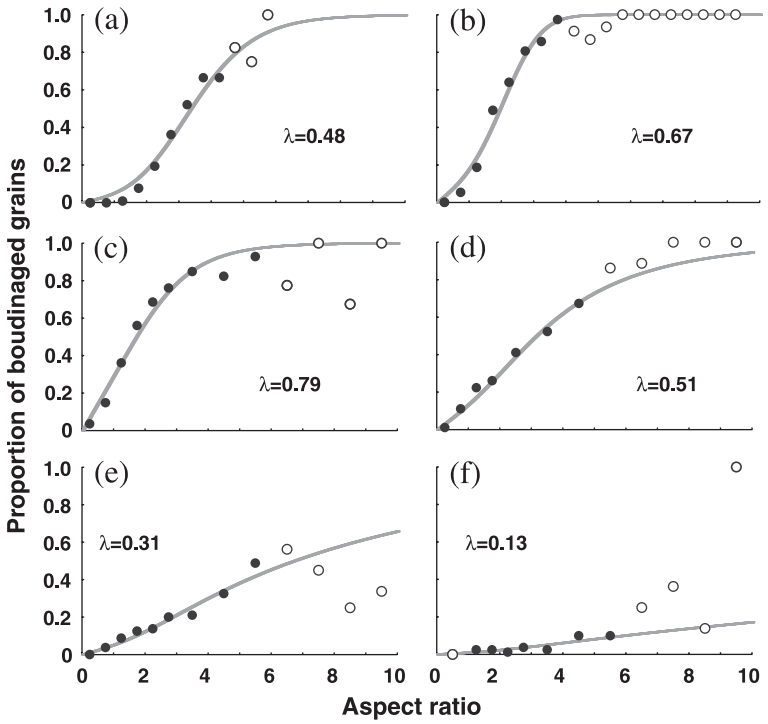

Fig. 6. Proportion of boudinaged grains with respect to aspect ratio. Tourmaline boudins were analysed for Wadi Tayin (a) and Greenbushes (b) samples. Piemontite boudins were reanalysed for the four samples analysed previously by Masuda et al. (1989): Nuporomaporo (c), Yamagami (d), Matsunosako (e) and Asemi (f). For details, see Masuda et al. (1989). Solid and open circles indicate reliable and unreliable data (>25 measured grains are regarded as reliable). The curve represents the best-fit $G(r, m, \lambda)$ using reliable data. The λ value of each sample is indicated in the diagram.

from Eq. (11) by substituting values of E_q, E_f and ν_m (Simmons and Wang, 1971) and assuming $R_0/r_0 = 10$. As A is proportional to $[\ln(R_0/r_0)]^{-1/2}$, the value of R_0/r_0 does not greatly influence the value of A. $R_0/r_0 = 10$ is valid as an approximation.

The Weibull modulus, m, is unknown for tourmaline and piemontite. As the influence of m on G in Eq. (12) is large, m was treated as an unknown parameter. The values of λ and m were derived simultaneously so as to minimise $T(m, \lambda)$ as follows.

$$T(m,\lambda) = \sum_r \left[G(r,m,\lambda) - M(r)\right]^2. \qquad (15)$$

By a least-square analysis of Eq. (15), $m = 4$ and 2 is obtained for tourmaline and piemontite, respectively. These values are in the range of typical ceramic materials (e.g., Petry et al., 1997). The best fit $G(r, m, \lambda)$ curve for each sample is shown in Fig. 6. The fitting of $G(r, m, \lambda)$ to $M(r)$ was evaluated by a χ^2-test with a critical region of 0.05 (e.g., Cheeney, 1983), and was found to be excellent.

6. Estimate of the magnitude of palaeo-stress

Using the above procedure, the value of λ can be determined uniquely for each sample. As $\sigma_0 = \lambda S^*$, quantification of S^* is required for estimating σ_0. S^* is not a constant for each mineral but varies with temperature, pressure and other conditions such as partial pressure of H_2O (e.g., Paterson, 1976). S^* even has a size effect that is critical in our analysis. Therefore, the same λ value for different samples does not indicate the same magnitude of differential stress. Evaluation of S^* is the next step in estimating the magnitude of differential stress by this method. Determination of m of fibre materials is another possible means of improving the microboudin

method. S^* and m should be analysed through experimental studies.

7. Summary

We refined the microboudin method to infer the relative magnitude of differential stress by incorporating a new shear-lag model for the relationship between far-field differential stress and differential stress transferred to the fibre. We successfully applied the refined method to tourmaline boudinage structures from Greenbushes (Western Australia) and Wadi Tayin (Oman), and obtained stress parameters for differential stress determination. We also successfully applied the method to piemontite microboudinage structures treated previously by Masuda et al. (1989). The magnitude of palaeo-differential stress can be estimated by this method if the fracture strength of tourmaline or piemontite is known.

Acknowledgements

We thank Shaocheng Ji for suggestions regarding our microboudin method, and Hideki Mori for preparing beautiful thin sections. We also thank J.-P. Burg, G. E. Lloyd and M. Jessell for constructive comments.

Part of this study was financially supported by a research grant to S. Miyashita and S. Arai from the Japan Society for the Promotion of Science.

Appendix A. Notation of important parameters

G	probability density function of fractured grains (theoretical)
M	proportion of microboudinaged grains (measured)
m	Weibull modulus
r	aspect ratio of fibre
E_q	Young's modulus of matrix
E_f	Young's modulus of fibre
B	stress parameter of the previous method (Masuda et al., 1989, 1990)
λ	stress parameter of the refined method (this paper)
σ_0	far-field differential stress
S^*	fracture strength of the fibre material at $r=1$

References

Boudier, F., Coleman, R.G., 1981. Cross section through the peridotite in the Semail ophiolite, southeastern Oman Mountains. J. Geophys. Res. 86, 2573–2592.

Cheeney, R.F., 1983. Statistical Methods in Geology. George Allen and Unwin, London.

Epstein, B., 1948. Statistical aspects of fracture problems. J. Appl. Phys. 19, 140–147.

Etheridge, M.A., Wilkie, J.C., 1981. An assessment of dynamically recrystallized grain size as a palaeopiezometer in quartz-bearing mylonite zones. Tectonophysics 78, 475–508.

Ferguson, C.C., 1981. A strain reversal method for estimating extension from fragmented rigid inclusions. Tectonophysics 79, T43–T52.

Hacker, B.R., Mosenfelder, J.L., 1996. Metamorphism and deformation along the emplacement thrust of the Samail ophiolite, Oman. Earth Planet. Sci. Lett. 144, 435–451.

Hacker, B.R., Mosenfelder, J.L., Gnos, E., 1996. Rapid emplacement of the Oman ophiolite: thermal and geochronologic constraints. Tectonics 15, 1230–1247.

Hobbs, B.E., Means, W.D., Williams, P.F., 1976. An Outline of Structural Geology. Wiley, New York. 571 pp.

Jamison, W.R., Spang, J.H., 1976. Use of calcite twin lamellae to infer differential stresses. Geol. Soc. Amer. Bull. 87, 868–872.

Kelly, A., 1973. Strong Solid. Clarendon Press, Oxford.

Lacombe, O., 2001. Paleostress magnitudes associated with development of mountain belts: Insights from tectonic analyses of calcite twins in the Taiwan Foothills. Tectonics 20, 834–849.

Lawn, B., 1993. Fracture of Brittle Solids, 2nd ed. Cambridge Univ. Press, Cambridge. 378 pp.

Lloyd, G.E., Ferguson, C.C., Reading, K., 1982. A stress-transfer model for the development of extension fracture boudinage. J. Struct. Geol. 4, 355–372.

Masuda, T., Shibutani, T., Igarashi, T., Kuriyama, M., 1989. Microboudin structure of piedmontite in quartz schists: a proposal for a new indicator of relative palaeodifferential stress. Tectonophysics 163, 169–180.

Masuda, T., Shibutani, T., Kuriyama, M., Igarashi, T., 1990. Development of microboudinage: an estimate of changing differential stress with increasing strain. Tectonophysics 178, 379–387.

Masuda, T., Shibutani, T., Yamaguchi, H., 1995. Comparative rheological behaviour of albite and quartz in siliceous schists revealed by the microboudinage of piedmontite. J. Struct. Geol. 17, 1523–1533.

Mercier, J.-C.C., Anderson, D.A., Carter, N.L., 1977. Stress in the lithosphere: inferences from steady state flow of rocks. Pure Appl. Geophys. 115, 199–226.

Ord, A., Christie, J.M., 1984. Flow stresses from microstructures in mylonitic quartzites of the Moine Thrust Zone, Assynt area, Scotland. J. Struct. Geol. 6, 639–654.

Partington, G.A., 1990. Environment and structural controls on the intrusion of the giant rare metal Greenbushes pegmatite, Western Australia. Econ. Geol. 85, 437–456.

Passchier, C.W., Trouw, R.A.J., 1996. Microtectonics. Springer, Berlin. 289 pp.

Petry, M.D., Mah, T.-I., Kerans, R.J., 1997. Validity of using

average diameter for determination of tensile strength and Weibull modulus of ceramic filaments. J. Am. Ceram. Soc. 80, 2741–2744.

Rowe, K.J., Rutter, E.H., 1990. Paleostress estimation using calcite twinning: experimental calibration and application to nature. J. Struct. Geol. 12, 1–17.

Sellars, C.M., 1978. Recrystallization of metals during hot deformation. Philos. Trans. R. Soc. Lond., A 288, 147–158.

Simmons, G., Wang, H., 1971. Single Crystal Elastic Constants and Calculated Aggregate Properties: A Handbook. MIT Press, Cambridge. 370 pp.

Taya, M., Arsenault, R.J., 1989. Metal Matrix Composites. Pergamon, Oxford. 264 pp.

Twiss, R.J., 1986. Variable sensitivity piezometric equations for dislocation density and subgrain diameter and their relevance to olivine and quartz. AGU Geophys. Monogr. 36, 247–261.

Weathers, M.S., Bird, J.M., Cooper, R.F., Kohlstedt, D.L., 1979. Differential stress determined from deformation-induced microstructures of the Moine Thrust Zone. J. Geophys. Res. 84, 7495–7509.

Weibull, W., 1939. Statistical theory of the strength of materials. Ing. Vetenskaps Akad. Handl. 151 (cited in Epstein, 1948).

White, S.H., Burrows, S.E., Carreras, J., Shaw, N.D., Humphreys, F.J., 1980. On mylonites in ductile shear zones. J. Struct. Geol. 2, 175–187.

Zhao, P., Ji, S., 1997. Refinements of shear-lag model and its applications. Tectonophysics 279, 37–53.